Toxicology 377 (2017) 64–72

Contents lists available at ScienceDirect

Toxicology

journal homepage: www.elsevier.com/locate/toxicol

Effects of chronic lead exposure on bone mineral properties in femurs of growing rats

Pedro Álvarez-Lloret[a,*], Ching Ming Lee[b], María Inés Conti[b], Antonela Romina Terrizzi[b], Santiago González-López[c], María Pilar Martínez[b]

[a] Departamento de Geología, Facultad de Geología, Universidad de Oviedo, Oviedo, Spain
[b] Universidad de Buenos Aires, Facultad de Odontología, Cátedra de Fisiología, Buenos Aires, Argentina
[c] Department of Operative Dentistry, School of Dentistry, University of Granada, Spain

ARTICLE INFO

Article history:
Received 28 September 2016
Received in revised form 19 November 2016
Accepted 27 November 2016
Available online 30 November 2016

Keywords:
Lead intoxication
Rat femur
Bone mineralization
Bone morphology
Bone turnover
Osteoporosis

ABSTRACT

Lead exposure has been associated with several defective skeletal growth processes and bone mineral alterations. The aim of the present study is to make a more detailed description of the toxic effects of lead intoxication on bone intrinsic material properties as mineral composition, morphology and microstructural characteristics. For this purpose, Wistar rats were exposed (n = 12) to 1000 ppm lead acetate in drinking water for 90 days while control group (n = 8) were treated with sodium acetate. Femurs were examined using inductively coupled plasma optical emission spectrometry (ICP-OES), Attenuated Total Reflection Fourier transform infrared spectroscopy (ATR-FTIR), X-ray diffraction (XRD), and micro-Computed Tomography (μCT). Results showed that femur from the lead-exposed rats had higher carbonate content in bone mineral and $(Ca^{2+} + Mg^{2+} + Na^{+})/P$ ratio values, although no variations were observed in crystal maturity and crystallite size. From morphological analyses, lead exposure rats showed a decreased in trabecular bone surface and distribution while trabecular thickness and cortical area increased. These overall effects indicate a similar mechanism of bone maturation normally associated to age-related processes. These responses are correlated with the adverse actions induced by lead on the processes regulating bone turnover mechanism. This information may explain the osteoporosis diseases associated to lead intoxication as well as the risk of fracture observed in populations exposed to this toxicant.

1. Introduction

Bone is a biological composite formed by a mineral phase, mainly carbonated apatite, and an organic matrix, mostly collagen. Bone mineral is hierarchically ordered on a specific spatial configuration and structure from nanometer to centimeter scale (Olszta et al., 2007). Bone formation and growth is controlled by a complex array of feedback processes that depends on several biological and environmental factors (i.e. exposure to toxicants). A number of toxicological studies have demonstrated that bone tissue is highly sensitive to many types of toxic substances (i.e., heavy metals, organochlorine compounds) which affect bone composition and mineralization, producing specific bone abnormalities and pathologies (Álvarez-Lloret et al., 2009; Hodgson et al., 2008; Rodríguez-Estival et al., 2013; Rodríguez-Navarro et al., 2006). Environmental Pb exposure has been associated with retarded skeletal growth (Berlin et al., 1995). As well, several studies in laboratory model have also described different pathological processes in bone tissue due to lead toxicity, as evidenced by decreased trabecular bone volume and thinner growth plate cartilage in growing laboratory animals (Conti et al., 2012b). In addition, Pb intoxication has been also shown to impair bone biomechanics and structure in ovariectomized rats, suggesting a deleterious effect of the metal in older stages of life (Lee et al., 2016).

Lead poisoning may exert both direct and indirect actions on the processes regulating bone turnover mechanisms (Berglund et al., 2000). These alterations are related to the compatibility of Pb^{2+} to substitute Ca^{2+} in the apatite lattice and, consequently, altering the homeostasis of calcium in bone metabolism. Moreover, lead exposure may alter hormonal regulation of organisms and directly damage bone-cells functions (Berglund et al., 2000). Previous studies have shown how lead exposure can alter the bone

* Corresponding author at: Departamento de Geología, Facultad de Geología, Campus de Llamaquique, Oviedo 33005, Asturias, Spain.
E-mail address: pedroalvarez@uniovi.es (P. Álvarez-Lloret).

http://dx.doi.org/10.1016/j.tox.2016.11.017
0300-483X/

mineral composition and affect bone maturation and skeletal growth (Monir et al., 2010; Rodríguez-Estival et al., 2013). Furthermore, many researches also demonstrated that increased lead exposure is also associated with decreased bone mineral density as well as detrimental bone strength (Escribano et al., 1997; Ronis et al., 2001). Lead intoxication is known to induce higher risk of fractures as it affects several biomechanical properties, such as maximal load supported at fracture and energy absorption capacity by the whole bone. Additionally, geometrical properties are also impaired after lead exposure, as reported by a diminished diaphyseal bone marrow medullar cavity in femur of growing rats (Conti et al., 2012a, 2012b). As there is an intimate connection between bone composition and morphology and bone biomechanical properties, the mineral composition should be taken into consideration when analyzing Pb effects on bone structure. It is also well known that lead, once absorbed into the body, is mainly stored (more than 95%) in the mineralized tissues (i.e., teeth and bones). Moreover, lead accumulation will occur predominately in trabecular bone during childhood, and in both cortical and trabecular bone in adulthood (Auf der heide and Wittmers, 1992). Therefore, the effects of lead accumulation in bone can be expressed in different ways in these regions determining the diverse response to chronic poisoning.

Although there is a high interest in the study of the metabolic and physiological alterations caused by lead exposure in organisms, few studies have focused on the detailed analysis of the changes produced by this exposure in bone tissue at mineral level and its properties. Several effects have been described on bone mineralization due to environmental lead exposure in species of ungulates and birds through different acquisitions and sources (Álvarez-Lloret et al., 2014; Gangoso et al., 2009; Rodríguez-Estival et al., 2013). Controlled animal studies have also showed significant alterations on bone mineralization in lead exposure in vivo models (Lee et al., 2016; Monir et al., 2010). In this sense, several analytical techniques are available to study the inorganic properties of bone tissue that also allow to identified specific toxic lead effects due to pathological conditions affecting bone mineralization.

The purpose of this research was to conduct a comprehensive analysis of the bone mineral composition, morphological and microstructure characteristics in femurs to study the effects of chronic lead poisoning in a Wistar rat model. The present study was designed with the same experimental model as the one proposed in previously reported studies from our laboratory (Conti et al., 2012a, 2012b) in which morphological alterations were observed but the material properties were not deeply investigated. For this purpose, we have employed a combination of analytical techniques including: inductively coupled plasma optical emission spectrometry (ICP-OES), Attenuated Total Reflection Fourier transform infrared spectroscopy (ATR-FTIR), X-ray diffraction (XRD), and micro-Computed Tomography (μCT) analyses to fully characterize bone mineral properties. The combined use of these techniques can provide detailed compositional and structural information of bone at different scales. This information may help us to define the specific mechanisms behind the toxic effects on bone mineralization provoked by lead exposure.

2. Materials and methods

2.1. Animal treatment and sample preparation

Twenty female Wistar rats aged 21 days from the animal facility of the Faculty of Pharmacy and Biochemistry, Buenos Aires University (Argentina), were used throughout the experiments. They were housed in stainless-steel cages and maintained under local vivarium conditions (temperature 22–23 °C, 12-h on/off light cycle). All animals were allowed free access to tap water and a standard Pb free pelleted chow diet. Tap water quality is in accordance with international guidelines and standards ISO and WHO references being the Pb content less than 0.005 ppm. Rats were randomly divided into 2 groups. Pb intoxication was induced in 12 animals through administration of 1000 ppm of lead acetate in the same tap water for 90 days (Hamilton and O'Flaherty, 1994). Control animals (n = 8) received equivalent acetate, as sodium acetate, added to the mentioned water. All animals were treated in accordance with the National Institutes of Health guidelines for the care and use of laboratory animals (NIH 8th edition, 2011). Protocols were approved by the Ethical Commission of the Faculty of Dentistry, University of Buenos Aires (N° 11/06/2012–23). Body weight and femur length were registered at the beginning of the experiment (day 0) and at the end of the experimental period (day 90). Animals were euthanized by unconscious decapitation and femurs were properly dissected, cleaned from soft tissue, and stored at −20 °C until analyses. For ICP-OES, ATR-FTIR, and DRX analyses bone samples were previously powdered using a cryogenic mill (CertiPrep 6750 Freezer/Mill, SPEX).

2.2. Elemental analyses

For the elemental analyses, 30 mg of bone powder was dissolved in a 10 ml solution of 70% HNO_3 (1 ml, 24 h) and 30% H_2O_2 (1 ml, 24 h) and microwave digested. Calcium, phosphorus, magnesium, sodium and lead concentrations were measured using an Optima 8300 ICP-OES (Perkin Elmer). Concentrations are given in dry weight (d.w.). The precision of chemical analyses was higher than 1 ppm.

2.3. Fourier transform infrared (ATR-FTIR) spectroscopy

For the ATR-FTIR analyses, infrared spectra were obtained on a FT/IR-6200 spectrometer (JASCO, Japan). Infrared spectra were collected from 600 to 4000 cm^{-1} in absorbance mode, 124 scans at 1 cm^{-1} resolution. All curve fitting was performed and integrated areas measured using the curve fitting software JASCO Spectra Manager ® and PeakFit v4.11 Systat Software Inc. Two different IR bone absorption regions (900–1200 cm^{-1} and 1300–1750 cm^{-1} bands) were analyzed by curve fitting for control and lead-exposed groups (Fig. 1). The amount of phosphate, carbonate and collagen in bone samples were estimated from the peak area of each absorption bands associated with phosphate, carbonate, amide and C—H aliphatic groups identified in the infrared spectra (Boskey et al., 1998; Boskey and Mendelsohn, 2005; Gadaleta et al., 1996; Paschalis et al., 1996; Rey et al., 1989). Overlapping peaks were resolved using a second derivative methodology and fitted to a mixed derivative Gaussian + Lorentzian function. Fig. 2 displays the curve-fitting analysis for average IR spectra for control group in the 900–1200 cm^{-1} (phosphate absorption bands) and 1300–1750 cm^{-1} (carbonate type B substitution and amides absorption bands). To minimize the effect of differences in sample size, peak areas were normalized to the area of 3800–2800 cm^{-1} band region associated with OH groups after removing the C—H stretching peak area from this region. All data were baseline corrected and expressed as intensities ratios. A detailed description of the methodology used in described elsewhere (Rodríguez-Navarro et al., 2006). The following parameters derived from the ATR-FTIR spectra analyses were calculated to describe bone mineral composition and crystallinity index parameters. The degree of bone mineralization was defined as the band intensity ratios of phosphate species in the bone mineral to organic matrix ratio (Pienkowski et al., 1997) and was estimated as follows: A900-1200/A1660; where A900-1200 represent the amount of phosphate in bone and A1660 the amount of amide I groups (main band from

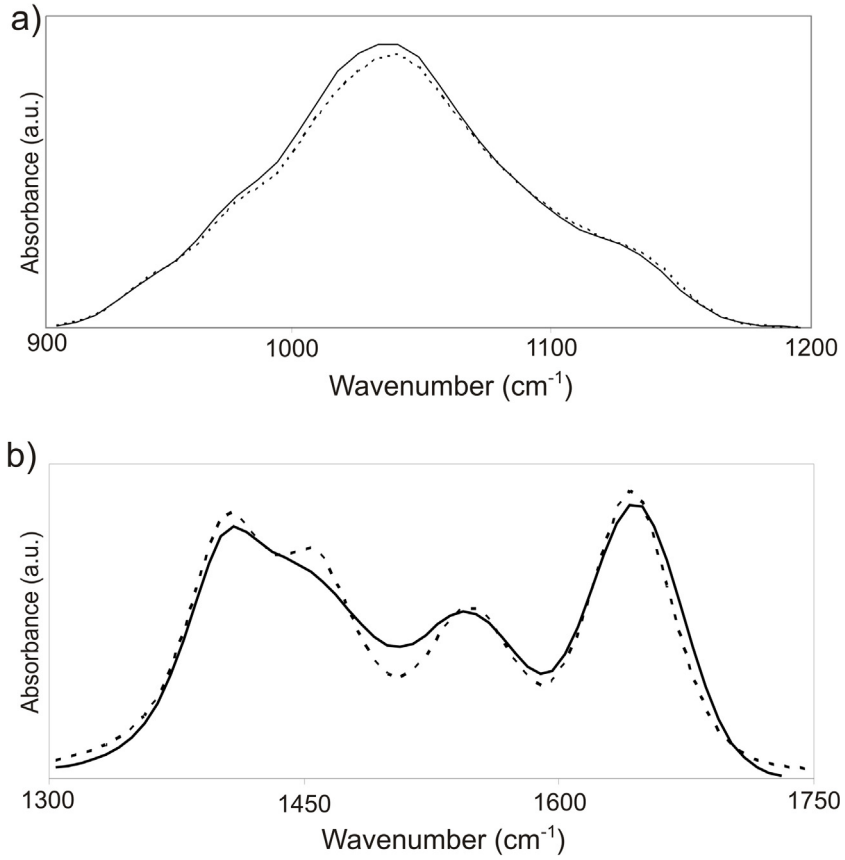

Fig. 1. Representative bone FTIR absorption spectra bands of control (solid line) and lead exposed (dotted line) rats in the regions: (a) 900–1200 cm^{-1} (phosphate group bands) and (b) 1300–1750 cm^{-1} (carbonate and amide group bands).

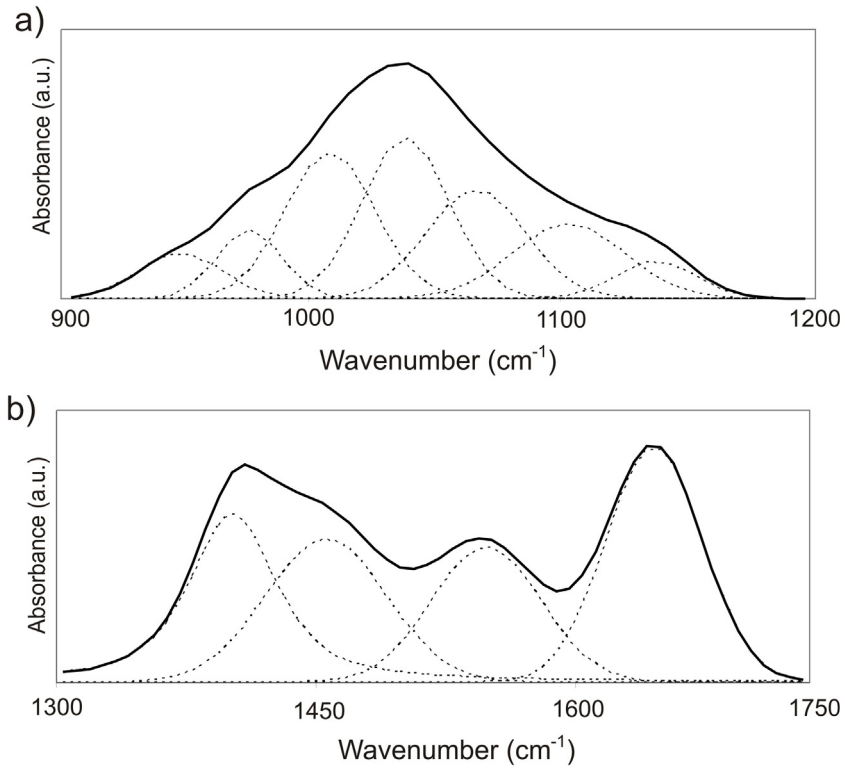

Fig. 2. Overlapping peaks deduced by curve-fitting analysis for average IR spectra for control group: (a) 900–1200 cm-1, band region associated with phosphate groups, and (b)1300–1750 cm^{-1} band region associated with different vibration modes for amide groups in collagen and carbonate groups (type B mineral substitution).

bone organic matrix; Boskey, 1999). The relative amount of carbonate in bone mineral (minCO3) was calculated as the ratio of the peak area at 1405 cm^{-1} (carbonate type B substitution, Rey et al., 1989) to phosphate band area (A900-1200). The crystallinity index (CI) was calculated as the ratio of the peak area at 1030 cm^{-1} (related with highly crystalline apatite) to 1010 cm^{-1} (poorly crystalline apatite; Miller et al., 2001).

2.4. Bone powder X-ray diffraction (XRD) analyses

X-ray diffraction was performed with an X'Pert Pro (PANalytical) powder diffractometer using CuKα radiation produced at 40 mA and 45 kV. Scans were performed between 2θ values of 20° and 75° with a step of 0.0042° and a count time/step of 5.08 s. The average crystallite size (D) of the apatite-bone crystals were calculated from (002) diffraction peak (apatite *c-axis*) using XPowder software (Martín-Ramos, 2004) by Scherrer equation (Schreiner and Jenkins, 1983):

$$D_{(002)} = K\,\lambda / B^{1}/_{2}\cos\theta \quad (1)$$

where K is the broadening constant varying with crystal habit and chosen as 0.9 for elongated apatite crystals (Klug and Alexander, 1959), λ is the wavelength CuKα radiation (λ = 1.5406 nm), $B^{1}/_{2}$ is the square root of the full width at half maximum (FWHM) of the 002 peak of apatite and θ is the corresponding diffraction angle. Crystallite size (D) is expressed in angstrom units (Å). The width of an XRD line represents a measure of the average coherent crystal size domains and can be employed as a crystallinity index of apatite bone crystals.

2.5. Microtomography analyses (μCT)

Microarchitecture of the femoral bone (3 femurs per group) was investigated using a high-resolution microcomputed tomograph (CT; Skyscan 1174; Skyscan BRUKER, Kontich, Belgium). The sample-holder device for μCT acquisition was used to fit the specimen with the long axis perpendicular to the floor of the specimen holder and the x-ray source. The X-ray source was set at 50 kV and 800 mA, with a pixel size at 17 μm. For each specimen, 465 projection images were acquired over an angular range of 180° (angular step of 0.40°). Flat field correction was performed at the beginning of each scan. The image slices were reconstructed using the cone-beam reconstruction software NRecon (Skyscan).

Morphometric analysis was based on the 2-D and 3-D internal CTAn plug-ins. Region of interest (ROI) was manually delimited in each of the samples. For the analysis of the diaphyseal cortical region 150 slices were chosen. Global grayscale threshold levels for this area were between 110 and 250. Growth place was chosen as reference point in all cases for cortical assessments. For the trabecular region a total of 150 slices were selected and adaptative grayscale threshold levels between 78 and 250 were used.

The following microarchitectural descriptors were examined for trabecular region: bone surface (BS), ratio of bone surface/bone volume (BS/BV), ratio of bone volume/tissue volume (BV/TV), trabecular thickness (Tb.Th), trabecular separation (Tb.Sp) and trabecular number (Tb.N). For the cortical region were determined: cortical bone area (Ct.Ar), total cross-sectional area (Tt.Ar), cortical area fraction (Ct.Ar/Tt.Ar), average cortical thickness (Ct.Th) and cortical porosity (Ct.Po). A detailed description of the parameters used is described elsewhere (Dempster et al., 2012).

2.6. Statistical analysis

Bone variables were expressed using means ± SD. Differences between groups were assessed by one-way ANOVA using the Fisher's LSD post hoc test. The level of significance chosen for all analyses was $p \leq 0.05$. Differences were considered significant at $p < 0.05$. Statistical analysis was performed using SPSS (SPSS Inc., Chicago, IL, USA).

3. Results

3.1. Development parameters

Development parameters are represented in Fig. 3. Experimental group (Pb) showed a significant reduction ($p < 0.01$) vs the

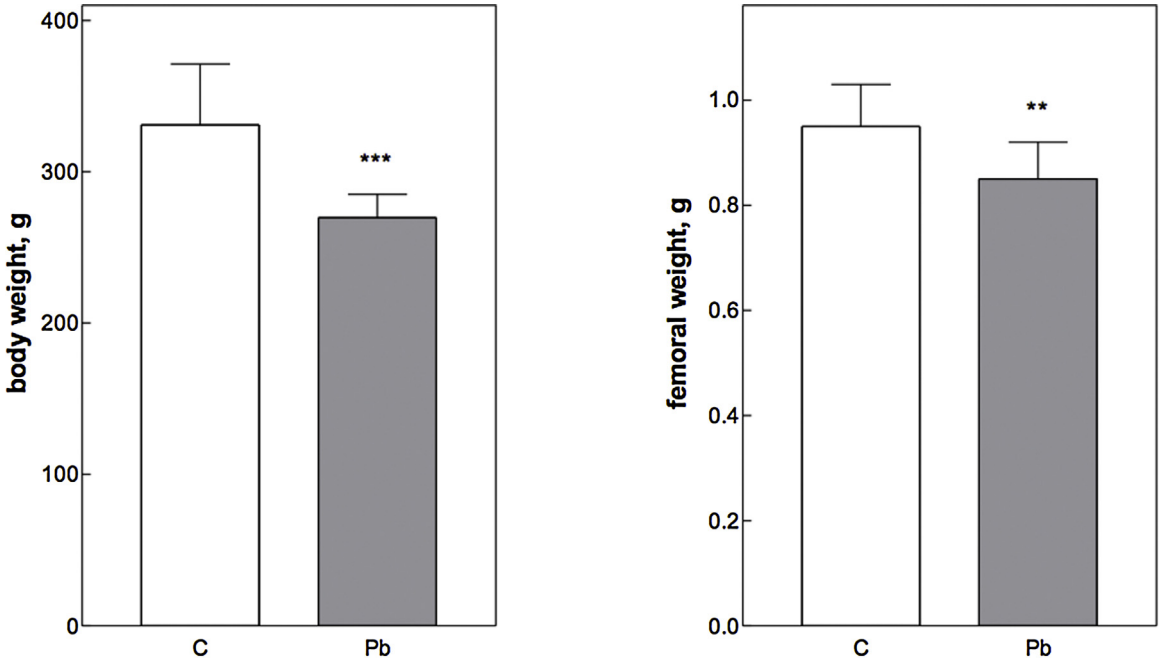

Fig. 3. Body (left) and femoral (right) weight measurements from Wistar rats exposed to lead (Pb) and control (C) group. Values are expressed as meand ± SD (**$p < 0.01$, ***$p < 0.001$).

control group (C) in body weight (267 ± 16 vs 331 ± 41) and in femoral weight (0.85 ± 0.07 vs 0.95 ± 0.08).

3.2. Elemental analyses

Bone elemental analyses are reported in Table 1. Bone elemental Ca, Mg, Na, and P contents did not significantly differ between groups. Lead content in exposure group indicated that the administered Pb was deposited in the skeleton in significant loads. A significant increment was found for (Ca + Mg + Na)/P ratio values between control and lead exposure group (p = 0.038).

3.3. Bone mineral composition and crystallinity properties

Table 2 shows the bone mineral composition and crystallinity properties of rat femora (XRD and ATR-FTIR analyses). The results from the ATR-FTIR analysis revealed a significant increase in the carbonate content in bone mineral in rats exposed to lead vs. control group (p = 0.012). The Crystallinity Index calculated from XRD (CI_{XRD}) data did not show any significant difference between the two groups. Nevertheless, CI_{XRD} was positively correlated (r = 0.566, p = 0.005) with Cristallinity Index obtained by FTIR analyses (Fig. 4 and 5) .

3.4. Morphometrical determinations

Bone micro-architectural parameters obtained by μCT analyses are reported in Table 3. Trabecular bone microarchitecture parameters in lead exposed rats show a significant decreased bone surface (BS; p = 0.025), ratio of bone surface/bone volume (BS/BV; p = 0.020) and an increased trabecular thickness (Tb.Th; p = 0.019) as compared with control group. Cortical bone micro-architecture showed significant increments in cortical area (Ct.Ar; p = 0.036) in lead exposure rats compared to control group.

Table 1
Elemental analyses measured by ICP-OES in the femurs of Wistar rats, control and lead exposure group. Values are expressed as Mean ± SD. (L.O.D. = limits of detection, NS = not significant).

	Control (n = 8)	Lead (n = 12)	P value
Pb (mg/L)	L.O.D	1,00 ± 0,07	
Ca (mg/L)	759 ± 204	693 ± 69	NS
Mg (mg/L)	13 ± 4	13 ± 3	NS
Na (mg/L)	22 ± 5	22 ± 4	NS
P (mg/L)	400 ± 113	354 ± 27	NS
Ca/P	1,91 ± 0,05	1,95 ± 0,06	NS
(Ca + Mg + Na)/P	1,99 ± 0,05	2,05 ± 0,06	0,038

Table 2
Bone parameter measured by ATR-FTIR and XRD for femurs in Wistar rats exposed to lead for 3 months. Values are Mean ± SD. (NS = not significant).

	Control (n = 8)	Lead (n = 12)	P value
ATR-FTIR analyses			
Total phosphate	47 ± 11	48 ± 12	NS
Total carbonate	9 ± 2	10 ± 2	NS
Degree of bone mineralization	4,7 ± 0,2	5,1 ± 0,9	NS
Carbonate in bone mineral	0,19 ± 0,01	0,22 ± 0,02	,012
Crystallinity index	0,58 ± 0,05	0,56 ± 0,06	NS
XRD analyses			
Crystallite size (Å)	154 ± 9	159 ± 12	NS

Fig. 3 displays μCT images showing the changes in cortical and trabecular distribution in control and lead exposed rat femurs. Cortical bone is dense and solid and surrounds the marrow space, whereas trabecular bone is composed by a honeycomb-like network of trabeculae plates and rods. Lead exposed femur (Fig. 3b) showed a marked loss of trabecular bone distribution from the metaphysic to the bone diaphysis compared with the distribution observed in control group sample (Fig. 3a).

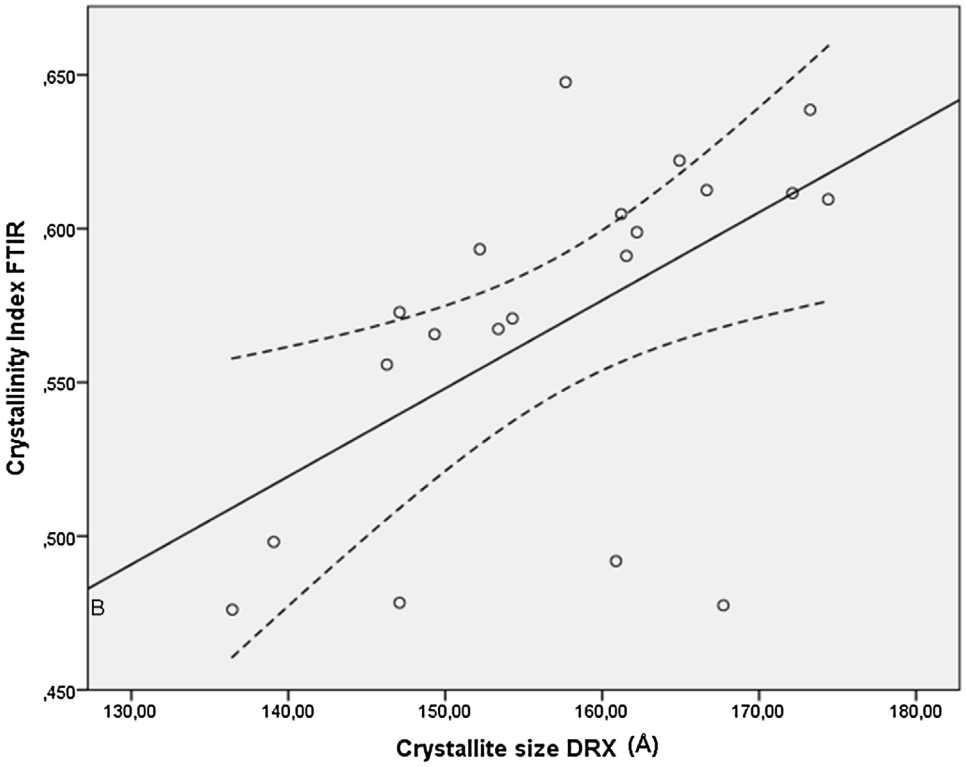

Fig. 4. Relationship between Crystallinity Indices, CIDRX and CIFTIR (n = 20, r = 0.566, p = 0.005). Regression lines with the 95% confidence intervals (dashed lines) are indicated.

Fig. 5. Micro-CT images showing the changes in cortical and trabecular distribution in femurs in (a) control (left) and (b) lead exposure (right) rats. Cortical bone is dense and solid whereas trabecular shows a honeycomb-like network. Note the marked loss of trabecular bone from the metaphysis to the bone diaphysis of exposed sample compared to control group.

Table 3
Bone micro-architectural parameters. Analyses were performed on trabecular and cortical bone in Wistar rat femurs in lead exposure and control group. Values are Mean ± SD (NS = non-significant).

	Control (n = 3)	Lead (n = 3)	P value
Trabecular			
BS (mm2)	275 ± 11	214 ± 28	0,025
BV/TV (%)	21 ± 2	20 ± 3	NS
BS/BV (1/mm)	49 ± 1	46 ± 1	0,020
Tb.Th (mm)	0,072 ± 0,001	0,078 ± 0,003	0,019
Tb.Sp (mm)	0,23 ± 0,02	0,28 ± 0,05	NS
Tb.N (1/mm)	3,0 ± 0,3	2,6 ± 0,4	NS
Cortical			
Ct.Ar (mm2)	4,7 ± 0,3	5,3 ± 0,2	0,036
Tt.Ar (mm2)	59 ± 1	59 ± 2	NS
Ct.Ar / Tt.Ar (%)	0,08 ± 0,01	0,09 ± 0,01	NS
Ct.Th (um)	512 ± 39	589 ± 42	NS
Ct.Po (mm3)	1,1 ± 0,4	0,8 ± 0,4	NS

4. Discussion

Many studies have shown the potential impact of lead exposure in the incidence of osteoporosis and the mechanisms involved in its toxic effects (Campbell et al., 2004; Escribano et al., 1997; Hamilton and O'Flaherty, 1994). In any case, less attention has been paid to the comprehensive effects provoked by lead exposure in bone mineral properties as well as how these alterations may affect to the bone quality and its characteristics (i.e. biomechanics). The current study gives additional information on the effects of chronic lead exposure on bone characteristics at several mineral scales (i.e. compositional, morphological and microstructural properties). The present research aimed to analyze the influence of lead intoxication on the impairment of long bone properties in growing Wistar rats exposed for 3 months. We demonstrate that several bone properties were affected by lead-exposed and the specific effects in bone mineral composition, microstructural properties, and morphology in femurs. Specifically, carbonate content in bone mineral and $(Ca^{2+} + Mg^{2+} + Na^{+})/P$ ratio values increased in rats exposed to lead, although no variations were observed in crystal maturity and perfection or crystallite size. Furthermore, at morphological level, lead exposure rats showed a decreased in trabecular bone surface and distribution while trabecular thickness and cortical area increased.

The mechanical bone properties strongly depend in the mineral characteristics of the bone tissue and its spatial distribution, that is to say, its geometrical properties (Ferretti, 1997). Previously reported studies from our laboratory (Conti et al., 2012a, 2012b) showed that chronic exposure to lead increases the risk of fracture in rat's femora, as a consequence of decreased maximal load supported at fracture and energy absorption capacity by the whole bone. In addition, these bones underwent different spatial organization compared to control animals, as the diaphyseal bone marrow medullar cavity was decreased, indicating that bone attempts to adapt the decline in the material properties. In this study, we developed morphometric analyses in femurs by μCT to fully characterize their cortical and trabecular bone structure, as these have shown to differ in composition (Ninomiya et al., 1990), remodeling time (Eriksen et al., 1993), and rate of metabolic

activity (Rico et al., 1994). As well, it has been also reported differences in the affinity for lead on trabecular and cortical bone (Christoffersson et al., 1987). From trabecular μCT analyses, the lowest bone surface and fraction of relative trabecular bone surface (BS and BS/BV values, Table 3) in the lead exposed group may be an indicator of an increased bone turnover. The trabecular bone is the mineral component more metabolically active and a lower proportion in bone tissue is related to higher rate of bone maturation (Clarke, 2008). In our research, the trabecular bone showed a loss in distribution from the metaphysis to the bone diaphysis in the lead exposed group (Fig. 5). These effects indicate a similar mechanism of bone maturation normally associated to age-related processes. These alterations may be attributed to a higher bone removal of trabeculae due to a dysregulation of bone metabolism (i.e. increased osteoclastic activity). In this sense, bone trabecular loss in osteoporotic and ageing is also accompanied by several topological changes in trabeculae microstructure properties, including the conversion of trabecular plates to rods (Wehrli, 2007). Similar effects have been reported in osteoporotic animals in which it was observable a considerable loss of trabecular bone distribution and a marked conversion of trabeculae into pillars (Legrand et al., 2007; Thompson et al., 1995). Although trabecular thickness is reduced by ageing and osteopororis these modifications in trabecular morphologies may be associated with the increased in trabecular thickness observed in lead-exposed bones in our research. Moreover, this phenomenon can be also related to the increased solubility rates of bone apatite with higher carbonate rates (Ito et al., 1997), as have been observed by FTIR analyses, being preferentially removed the trabecular morphologies with specific chemical composition and/or dimensions. As well, the deterioration of the bone trabeculae architecture and distribution results in a more anisotropic structure which has a greater susceptibility to fracture (McDonnell et al., 2007). In fact, a combination of different microdamage remodeling, adaptative and metabolic mechanisms has been proposed to relate the bone-loss at trabecular level with this anisotropic trabeculae organization. On the other hand, the femoral cortical increments in the cortical area (Ct.Ar) found in our experimental rats could be interpreted as an attempt of bone to compensate the loss of trabeculae trying to adapt the bone geometry to the new mechanical setting (Ferretti et al., 2003). In this sense, bone geometrical features changes with ageing adapting to a modified mechanical environment (Augat and Schorlemmer, 2006). This possible deterioration of intrinsic mechanical properties in bone may be directly related to the bone remodeling process (Currey et al., 1996). In fact, lead poisoning directly affects the bone cell functions (i.e. osteoclasts and osteoblasts) which play a key role during mineral maturation in bone metabolism. Overall, the bone remodeling process regulates the gain and loss of bone mineral density and directly influences bone strength (Clarke, 2008). Furthermore, these different responses in cortical and trabecular components in bone tissue, and its relationship with bone material characteristics, may contribute to the global mechanical properties of bone.

In addition, FT-IR spectroscopy is one of the major techniques for the qualitative and quantitative determination of the biochemical constituents in tissues and organs (Boskey and Mendelsohn, 2005; Severcan et al., 2005; Palaniappan and Vijayasundaram, 2009). Previous studies have demonstrated a decrease in the degree of mineralization, obtained by FT-IR spectroscopy, in bones exposed to lead poisoning (Álvarez-Lloret et al., 2014; Gangoso et al., 2009). Monir et al., 2010 also showed that lead exposure significantly alters several bone mineral composition characteristics (e.g. mineral/matrix, collagen maturity, crystallinity) measured by FTIRM. In our study, we have observed a higher carbonate in bone mineral in lead exposed rats compared to control group (Table 2). This substitution of phosphate by carbonate groups in bone mineral composition generally occurs during tissue ageing (Boskey and Pleshko Camacho, 2007; Magne et al., 2001). Thus, this compositional change in carbonate mineral content suggests increased bone maturation rate induced by lead exposure. This effect could be due to an alteration in bone remodeling rate affecting osteoblast and osteoclast functions (Pounds et al., 1991). Similar effects on carbonate mineral substitution were also previously observed in low- and high-turnover bone mechanisms, commonly occurs during osteoporosis disease (Boskey et al., 2005). Moreover, high rates carbonate-substitution in bone mineral hydroxyapatite has been associated to increased bone dissolution and related to fracture events in iliac crest biopsias (Gourion-Arsiquaud et al., 2013).

On the other hand, Ca/P ratio has been shown to be a sensitive measure of bone mineral quality (Tzaphlidou, 2008). It is also known that bone mineral contains variable amounts of Na^+ and Mg^{2+} cations in its composition (Driessens, 1980). In the current research, these cation concentrations were added to calcium in the Ca/P ratio values in order to obtain a more accurate measure of bone mineral quality parameter. This Ca/P ratio, as crystal size and CO_3^{-2} ion content, has demonstrated to increase with ageing (Legros et al., 1987). In this study, the increase in the $(Ca^{2+} + Mg^{2+} + Na^+)/P$ ratio in exposed rats (Table 1) is suggestive of an alteration in bone mineralization mechanisms with lead poisoning. These findings are in agreement with FTIR observations (i.e. carbonate content in bone mineral) which confirm a higher maturation rate in bone mineralization due to Pb exposure. XXX

Furthermore, the ability of apatite structure to accept lead ions can affect several crystalline properties of the bone mineral (Dowd et al., 2001). In our study, the Ca^{2+} ionic substitution by Pb^{2+} in the carbonated apatite structure have not shown any significant change in the crystallinity properties (related to the crystallite size/domain, $-CI_{RXD}$-, and mineral maturity, CI_{FTIR}) between groups. In any case, CI_{RXD} and CI_{FTIR} values were well correlated, indicating a direct relationship between crystalline environment mineral composition and crystallite apatite size (Fig. 4). Nevertheless, it has been previously demonstrated that the average sizes of apatite crystals increased with higher turnover rates, associated to bone-ageing (Boskey et al., 2005). Despite the fact that lead incorporation in the bone mineral seems not to modify the microstructure properties of apatite crystals, this chemical replacement may determine bone structural and/or morphological characteristics. As well, this ionic mechanism of bivalent cations substitution in bone apatite may also affect various fundamental biological processes (Berglund et al., 2000; Lidsky and Schneider, 2003) related to lead toxicity.

The mechanism of lead toxic effects on bone mineralization most likely involves multiple metabolic processes (Berglund et al., 2000). Lead intoxication has been previously related with the appearance of osteoporosis disease (Campbell and Auinger, 2007). Likewise, osteoporosis is characterized by a reduction in bone mass associated with altered bone quality correlated to a detrimental strength of bone biomechanics leading to an increasing risk of fracture (Lupsa and Insogna, 2015). The mechanical bone properties strongly depend in the geometrical properties, being those related to the spatial distribution of the mineralized tissues. As well, bone compositional and microstructural properties have been related to bone mechanical properties (Eriksen et al., 1993; Rey et al., 2009). In our study, the overall alterations in morphological, structural and bone compositional properties (carbonate mineral content, cortical area, trabecular bone surface, thickness and distribution) may reach a significantly counterproductive effect on biomechanical properties and bone quality. These effects may be correlated with the adverse actions induced by lead on the processes regulating bone turnover mechanisms and affecting bone maturation and skeletal growth (Berglund et al.,

2000; Palaniappan et al., 2010). Likewise, Monir et al., 2010 also observed significantly increased in the bone formation and resorption markers suggesting increased bone turnover. In this sense, Pb exposure may exert both direct (i.e. altering osteoclast and osteoblast cell functions) and indirect (via kidney dysfunction) actions on bone metabolism (Berglund et al., 2000). These metabolic disruption mechanisms may explain the effects observed in the current research on bone mineral characteristics. It also worth mentioning that the application of complementary analytical techniques to fully characterize the bone mineral component at different scales (i.e. compositional, morphological and microstructural) constitutes a suitable procedure to offer insights into possible toxic effects of lead exposure. Our results show how lead exposure for 3 months to Wistar rats provoked several responses in bone tissue mineralization that could be mediated by an alteration on bone turnover mechanisms processes involved in the mineral remodelation. This information may explain the osteoporosis diseases associated to lead intoxication as well as the risk of fracture observed in populations exposed to this toxicant.

Conflict of interest

The authors declare no conflict of interest.

Acknowledgments

We thank “Centro de Instrumentación Científica” (University of Granada, Spain) and “Servicios Científico Técnicos” (University of Oviedo, Spain) and the staff for their technical support and assistance. The authors also acknowledge the collaboration of Vanessa Loredo in μCT data analyses and processing. This study has been funded by projects CGL2011-25906 and CGL2015-64683-P (Ministerio de Economía y Competitividad, Spain) and UBACYT project 2016, N° 20020150100006BA (Universidad de Buenos Aires, Argentina).

References

Álvarez-Lloret, P., Lind, P.M., Nyberg, I., Orberg, J., Rodríguez-Navarro, A.B., 2009. Effects of 3,3',4,4',5-pentachlorobiphenyl (PCB126) on vertebral bone mineralization and on thyroxin and vitamin D levels in Sprague-Dawley rats. Toxicol. Lett. 187, 63–68.

Álvarez-Lloret, P., Rodríguez-Navarro, A.B., Romanek, C.S., Ferrandis, P., Martínez-Haro, M., Mateo, R., 2014. Effects of lead shot ingestion on bone mineralization in a population of red-legged partridge (*Alectoris rufa*). Sci. Total Environ. 466–467, 34–39.

Auf der heide, A.C., Wittmers Jr., L.E., 1992. Selected aspects of the spatial distribution of lead in bone. Neurotoxicol 13, 809–820.

Augat, P., Schorlemmer, S., 2006. The role of cortical bone and its microstructure in bone strength. Age Ageing 35, ii27–ii31.

Berglund, M., Åkesson, A., Bjellerup, P., Vahter, M., 2000. Metal-bone interactions. Toxicol. Lett. 112-113, 219–225.

Berlin, K., Gerhardsson, L., Börjesson, J., Lindh, E., Lundström, N., Schütz, A., Skerfving, S., Edling, C., 1995. Lead intoxication caused by skeletal disease. Scand. J. Work Environ. Health 21, 296–300.

Boskey, A.L., Mendelsohn, R., 2005. Infrared spectroscopic characterization of mineralized tissues. Vib. Spectrosc. 38, 107–114.

Boskey, A., Pleshko Camacho, N., 2007. FT-IR imaging of native and tissue-engineered bone and cartilage. Biomaterials 28, 2465–2478.

Boskey, A.L., Gadaleta, S., Gundberg, C., Doty, S.B., Ducy, P., Karsenty, G., 1998. Fourier transform infrared microspectroscopic analysis of bones of osteocalcin-deficient mice provides insight into the function of osteocalcin. Bone 23, 187–196.

Boskey, A.L., DiCarlo, E., Paschalis, E., West, P., Mendelsohn, R., 2005. Comparison of mineral quality and quantity in iliac crest biopsies from high- and low-turnover osteoporosis: an FT-IR microspectroscopic investigation. Osteoporos. Int. 16, 2031–2038.

Campbell, J.R., Auinger, P., 2007. The association between blood lead levels and osteoporosis among adults–results from the third national health and nutrition examination survey (NHANES III). Environ. Health Perspect. 115, 1018–1022.

Campbell, J.R., Rosier, R.N., Novotny, L., Puzas, J.E., 2004. The association between environmental lead exposure and bone density in children. Environ. Health Perspect. 112, 1200–1203.

Christoffersson, J.O., Schutz, A., Skerfving, S., Ahlgren, L., Mattsson, S., 1987. A model describing kinetics of lead in occupationally exposed workers. In: Ellis, K.J., Yasumura, S., Morgan, W.D. (Eds.), In Vivo Body Composition Studies. Institute of Physical Sciences in Medicine, London, pp. 334–347.

Clarke, B., 2008. Normal bone anatomy and physiology. Clin. J. Am. Soc. Nephrol. 3, S131–S139.

Conti, M.I., Terrizzi, A.R., Lee, C.M., Mandalunis, P.M., Bozzini, C., Piñeiro, A.E., Martinez, M.P., 2012a. Effects of lead exposure on growth and bone biology in growing rats exposed to simulated high altitude. Bull. Environ. Contam. Toxicol. 88, 1033–1037.

Conti, M.I., Bozzini, C., Facorro, G., Lee, C.M., Mandalunis, P.M., Piehl, L., Piñeiro, A.E., Terrizzi, A.R., Martínez, M.P., 2012b. Lead bone toxicity in growing rats exposed to chronic intermittent hypoxia. Bull. Environ. Contam. Toxicol. 89, 693–698.

Currey, J.D., Brear, K., Zioupos, P., 1996. The effects of ageing and changes in mineral content in degrading the toughness of human femora. J. Biomech. 29, 257–260.

Dempster, D.W., Compston, J.E., Drezner, M.K., Glorieux, F.H., Kanis, J.A., Malluche, H., Meunier, P.J., Ott, S.M., Recker, R.R., Parfitt, A.M., 2012. 2013. Standardized nomenclature, symbols, and units for bone histomorphometry: a update of the report of the ASBMR Histomorphometry Nomenclature Committee. J. Bone Miner. 28, 2–17 (Res).

Dowd, T.L., Rosen, J.F., Mints, L., Gundberg, C.M., 2001. The effect of Pb2+ on the structure and hydroxyapatite binding properties of osteocalcin. BBA-Mol. Basis Dis. 1535, 153–163.

Driessens, F.C., 1980. Probable phase composition of the mineral in bone. Z. Naturforsch. C. 35, 357–362.

Eriksen, E.F., Vesterby, A., Kassem, M., Melsen, F., Mosekilde, L., 1993. Bone remodeling and bone structure. In: Mundy, G.R., Martin, T.J. (Eds.), Physiology and Pharmacology of Bone. Springer-Verlag, Berlin, pp. 67–109.

Escribano, A., Revilla, M., Hernández, E.R., Seco, C., González-Riola, J., Villa, L.F., Rico, H., 1997. Effect of lead on bone development and bone mass A morphometric, densitometric, and histomorphometric study in growing rats. Calcified Tissue Int. 60, 200–203.

Ferretti, J.L., Cointry, G.R., Capozza, R.F., Frost, H.M., 2003. Bone mass, bone strength, muscle-bone interactions, osteopenias and osteoporoses. Mech. Ageing Dev. 124, 269–279.

Ferretti, J.L., 1997. Biomechanical properties of bone. From Osteoporosis and Bone Densitometry. Springer, Berlin, pp. 143–161.

Gadaleta, S.J., Paschalis, E.P., Betts, F., Mendelsohn, R., Boskey, A.L., 1996. Fourier transform infrared spectroscopy of the solution mediated conversion of amorphous calcium phosphate to hydroxyapatite: new correlations between X-ray diffraction and infrared data. Calcified Tissue Int. 58, 9–16.

Gangoso, L., Álvarez-Lloret, P., Rodríguez-Navarro, Alejandro A.B., Mateo, R., Hiraldo, F., Donázar, J.A., 2009. Long-term effects of lead poisoning on bone mineralization in vultures exposed to ammunition sources. Environ. Pollut . 157, 569–574.

Gourion-Arsiquaud, S., Lukashova, L., Power, J., Loveridge, N., Reeve, J., Boskey, A.L., 2013. Fourier transform infrared imaging of femoral neck bone: reduced heterogeneity of mineral-to-matrix and carbonate-to-phosphate and more variable crystallinity in treatment-naive fracture cases compared with fracture-free controls. J. Bone Miner. Res. 28, 150–161.

Hamilton, J.D., O'Flaherty, E.J., 1994. Effects of lead exposure on skeletal development in rats. Fundam. Appl. Toxicol. 22, 594–604.

Hodgson, S., Thomas, L., Fattore, E., Lind, P.M., Alfven, T., Hellström, L., Håkansson, H., Carubelli, G., Fanelli, R., Jarup, L., 2008. Bone mineral density changes in relation to environmental PCB exposure. Environ. Health Perspect. 116, 1162–1166.

Ito, A., Maekawa, K., Tsutsumi, S., Ikazaki, F., Tateishi, T., 1997. Solubility product of OH-carbonated hydroxyapatite. J. Biomed. Mater. Res. 36, 522–528.

Klug, H.P., Alexander, L.E., 1959. X-Ray Diffraction Procedures. John Willey, New York, USA.

Lee, C.M., Terrizzi, A.R., Bozzini, C., Piñeiro, A.E., Conti, M.I., Martínez, M.P., 2016. Chronic lead poisoning magnifies bone detrimental effects in an ovariectomized rat model of postmenopausal osteoporosis. Exp. Toxicol. Pathol. 68, 47–53.

Legrand, E., Audran, M., Guggenbuhl, P., Levasseur, R., Chalès, G., Baslé, M.F., Chappard, D., 2007. Trabecular bone microarchitecture is related to the number of risk factors and etiology in osteoporotic men. Microsc. Res. Tech. 70, 952–959.

Legros, R., Balmain, N., Bonel, G., 1987. Age-related changes in mineral of rat and bovine cortical bone. Calcified Tissue Int. 41, 137–144.

Lidsky, T.I., Schneider, J.S., 2003. Lead neurotoxicity in children: basic mechanisms and clinical correlates. Brain 126, 5–19.

Lupsa, B.C., Insogna, K., 2015. Bone health and osteoporosis. Endocrin. Metab. Clin. 44, 517–530.

Magne, D., Pilet, P., Weiss, P., Daculsi, G., 2001. Fourier transform infrared microspectroscopic investigation of the maturation of nonstoichiometric apatites in mineralized tissues: a horse dentin study. Bone 29, 547–552.

Martín-Ramos, J.D., 2004. Using XPowder: A software package for powderX-ray diffraction analysis. GR1001/04. ISBN 84–609-1497-6

McDonnell, P., McHugh, P.E., O'Mahoney, D., 2007. Vertebral osteoporosis and trabecular bone quality. Ann. Biomed. Eng. 35, 170–189.

Miller, L.S., Vairavamurthy, V., Chance, M.R., Mendelsohn, R., Paschalis, E.P., Betts, F., Boskey, A.L., 2001. In situ analysis of mineral content and crystallinity in bone using infrared micro-spectroscopy of the v4 PO4- vibration. Biochim. Biophys. Acta 1527, 11–19.

Monir, A.U., Gundberg, C.M., Yagerman, S.E., van der Meulen, M.C., Budell, W.C., Boskey, A.L., Dowd, T.L., 2010. The effect of lead on bone mineral properties from female adult C57/BL6 mice. Bone 47, 888–894.
Ninomiya, J.T., Tracy, R.P., Calore, J.D., Gendreau, M.A., Kelm, R.J., Mann, K.G., 1990. Heterogeneity of human bone. J. Bone Miner. Res. 5, 933–938.
Olszta, M.J., Cheng, X., Jee, S.S., Kumar, R., Kim, Y.-Y., Kaufman, M.J., Douglas, E.P., Gower, L.B., 2007. Bone structure and formation: a new perspective. Mater. Sci. Eng. R-Rep. 58, 77–116.
Palaniappan, P.L.R.M., Vijayasundaram, V., 2009. The FT-IR study of the brain tissue of Labeo rohita due to arsenic intoxication. Microchem. J. 91, 118–124.
Palaniappan, P.L., Krishnakumar, N., Vadivelu, M., Vijayasundaram, V., 2010. The study of the changes in the biochemical and mineral contents of bones of Catla catla due to lead intoxication. Environ. Toxicol. 25, 61–67.
Paschalis, E.P., Jacenko, O., Olsen, B., Mendelsohn, R., Boskey, A.L., 1996. Fourier transform infrared microspectroscopic analysis identifies alterations in mineral properties in bones from mice transgenic for type X collagen. Bone 19, 151–156.
Pienkowski, D., Doers, T.M., Monier-Faugere, M.-C., Geng, Z., Camacho, N.P., Boskey, A.L., Malluche, H.H., 1997. Calcitonin alters bone quality in beagle dogs. J. Bone Miner. Res. 12, 1936–1943.
Pounds, J.G., Long, G.J., Rosen, J.F., 1991. Cellular and molecular toxicity of lead in bone. Environ. Health Perspect. 91, 17–32.
Rey, C., Collins, B., Goehl, T., Dickson, I.R., Glimcher, M.J., 1989. The carbonate environment in bone mineral: a resolution-enhanced Fourier Transform Infrared Spectroscopy study. Calcified Tissue Int. 45, 157–164.
Rey, C., Combes, C., Drouet, C., Glimcher, M.J., 2009. Bone mineral: update on chemical composition and structure. Osteoporos. Int. 20, 1013–1021.
Rico, H., Hernandez, E.R., Seco, C., Villa, L.F., Fernandez, S., 1994. Quantitative peripheral computed tomodensitometric study of cortical and trabecular bone mass in relation to menopause. Maturitas 18, 183–189.
Rodríguez-Estival, J., Álvarez-Lloret, P., Rodríguez-Navarro, A.B., Mateo, R., 2013. Chronic effects of lead (Pb) on bone properties in red deer and wild boar: relationship with vitamins A and D3. Environ. Pollut. 174, 142–149.
Rodríguez-Navarro, A.B., Romanek, C.S., Alvarez-Lloret, P., Gaines, K.F., 2006. Effect of in ovo exposure to PCBs and Hg on Clapper Rail bone mineral chemistry from a contaminated salt marsh in coastal Georgia. Environ. Sci. Technol. 15, 4936–4942.
Ronis, M.J., Aronson, J., Gao, G.G., Hogue, W., Skinner, R.A., Badger, T.M., Lumpkin Jr., C.K., 2001. Skeletal effects of developmental lead exposure in rats. Toxicol. Sci. 62, 321–329.
Schreiner, W.N., Jenkins, R., 1983. Profile fitting for quantitative analysis in X-ray powder diffraction. Adv. X-Ray Anal. 26, 141–147.
Severcan, F., Gorgulu, G., Gorgulu, S.T., Guray, T., 2005. Rapid monitoring of diabetes-induced lipid peroxidation by Fourier transform infrared spectroscopy: evidence from rat liver microsomal membranes. Anal. Biochem. 339, 36–40.
Thompson, D.D., Simmons, H.A., Pirie, C.M., Ke, H.Z., 1995. FDA Guidelines and animal models for osteoporosis. Bone 17, 125S–133S.
Tzaphlidou, M., 2008. Bone architecture: collagen structure and calcium/phosphorus maps. J. Biol. Phys. 34, 39–49.
Wehrli, F.W., 2007. Structural and functional assessment of trabecular and cortical bone by micro magnetic resonance imaging. J. Magn. Reson. I. 25, 390–409.